

Document downloaded from:

<http://hdl.handle.net/10251/122223>

This paper must be cited as:

Espinosa-López, J.C.; Navalón Oltra, S.; Alvaro Rodríguez, M.M.; Dhakshinamoorthy, A.; García Gómez, H. (2018). Reduction of C=C Double Bonds by Hydrazine Using Active Carbons as Metal-Free Catalysts. *ACS Sustainable Chemistry & Engineering*. 6(4):5607-5614. <https://doi.org/10.1021/acssuschemeng.8b00638>



The final publication is available at

<http://doi.org/10.1021/acssuschemeng.8b00638>

Copyright American Chemical Society

Additional Information

Reduction of C=C Double Bonds by Hydrazine using Active Carbons as Metal-Free Catalysts

Juan Carlos Espinosa,^a Sergio Navalon,^a Mercedes Alvaro,^a Amarajothi Dhakshinamoorthy,^{*b} Hermenegildo Garcia^{*a,c}

^a Departamento de Química and Instituto Universitario de Tecnología Química Consejo Superior de Investigaciones Científicas-Universitat Politècnica de Valencia, Universitat Politècnica de València, Av. De los Naranjos s/n, 46022, Valencia, Spain. E-mail: hgarcia@qim.upv.es

^b School of Chemistry, Madurai Kamaraj University, Palkalai Nagar, Madurai 625 021, Tamil Nadu, India. E-mail: admguru@gmail.com

^c Centre of Excellence for Advanced Materials Research, King Abdulaziz University, Jeddah, Saudi Arabia.

Abstract

A series of active carbons with or without chemical oxidation by nitric acid have been prepared and their activity was evaluated as metal-free catalysts for the C=C double bond hydrogenation using hydrazine as reducing agent in the presence of oxygen. It was observed that an optimal treatment by nitric acid results in a sample with enhanced catalytic activity that is superior to that measured under the same conditions for the other carbon materials. Kinetic data suggest that the active sites in the process could be quinone/hydroquinone type redox centres introduced in the oxidative treatment of AC by nitric acid. Nitric acid-oxidized active carbon has a wide substrate scope and also exhibits a chemoselective C=C hydrogenation with respect to nitro group reduction compared to conventional Pd/C.

Keywords: heterogeneous catalysis; carbocatalysis; active carbon; hydrazine; olefin reduction

Introduction

Catalysis is currently dominated by the use of transition metals, in many cases precious noble metals.¹⁻³ One current tendency in catalysis is to find alternatives to the use of critical metals used in the preparation of catalysts, replacing them by more abundant transition metals or even by metal-free catalysts.^{4,5} In this regard, the use of carbon catalysts is attracting considerable attention and one of the targets being to show the scope of this type of catalysts and particularly to apply them in reactions typically carried out by transition metals.⁶⁻⁸ In this context, the use of activated carbons as catalysts in the absence of added transition metals was known since long time ago, but mainly limited to the oxidation of pollutants, particularly NO_x in gas-phase.^{9, 10} Due to its wide availability and sustainability, active carbons coming from biomass waste are appealing materials to develop metal-free catalysts.^{10, 11} Within this line, one of the targets is to show that catalysts based on active carbons can promote reactions that up to now are almost exclusively catalysed by noble metals.^{12, 13}

One paradigmatic example metal catalyzed reactions is hydrogenation of C=C double bonds that is typically promoted by Pt, Pd, Rh and other noble metals, being of interest to develop alternatives based on metal-free catalysts. Very recently, following the work of Su and co-workers with carbon nanotubes,^{14, 15} it has been reported that graphitic carbon can act as metal free catalysts for hydrogenation of nitrobenzene using hydrazine as reducing agent.^{16, 17} Continuing with this line of research, herein we report that chemical oxidation of commercial active carbons increases their activity for hydrogenation of C=C double bonds by hydrazine. The leading idea based on the proposals of nature of active sites is that the modification of commercial carbon by chemical oxidation should improve the catalytic activity of this active carbon. As it has been proposed that carbonylic compounds, vicinal diketones at the periphery and defects of graphenic walls could be the active sites to activate

hydrazine,¹⁷ it can be speculated that oxidation of active carbons with nitric acid should be a favourable treatment to enhance the activity of these materials for hydrazine activation. The present manuscript provides experimental support to this hypothesis.

Experimental Section

Materials

Graphite (Aldrich, CAS 7782-42-5), diamond nanoparticles (ref: 636444, $\geq 97\%$), activated carbon (AC, Norit SX Ultra, ref. 53663) and palladium supported on activated carbon (Sigma Aldrich, ref.: 205699) were provided by Sigma Aldrich. Other reagents employed were analytical or HPLC grade were also provided by Sigma-Aldrich.

Catalyst preparation

AC catalysts treated with nitric acid were obtained by submitting the commercial AC sample to nitric acid oxidation. 1 g of AC (Norit SX Ultra) was dispersed in 25 mL HNO₃ (J.T. Baker, 65%) in a round bottom flask, and the mixture was heated in stirring at 83 °C for 3, 6 and 20 h as required. Then, this suspension was centrifuged at 12000 rpm and repeatedly washed with water until the supernatant liquid was neutral. The weight loss observed for AC-3, AC-6 and AC-20 catalysts were 7, 8.4 and 8.4 wt%, respectively. The samples obtained by this treatment were named AC-X (X being the time of the nitric acid treatment in hours). Graphene was prepared as previously reported by pyrolysis of sodium alginate at 900 °C under argon atmosphere.¹⁸ Briefly, 200 mg of sodium alginate were placed on a ceramic crucible inside a horizontal tubular (5 cm diameter, 90 cm length) electrical quartz furnace that was continuously flashed with argon (1 mL/minute).

AC-6 Derivatization

The AC-6 catalyst was submitted to different derivatization processes. AC-6=NPh was obtained by dispersing 200 mg of AC-6 with 100 μ L of benzylamine in 20 mL of distilled water by sonication in a round bottom flask. The mixture was set to pH 5 and stirred

magnetically for 24 h at 40 °C. After that, the sample was washed with Milli-Q water for several times, recovering the solid in each washing cycle by centrifugation. Finally it was washed with ethanol and recovered by filtration. AC-6_CO₂Me was obtained by dispersing 200 mg of AC-6 (prior drying in an oven at 100 °C for 12 h) in 10 mL of thionyl chloride in a two necked round bottom flask. The mixture was stirred and heated at 50 °C for 4 h. After that, the thionyl chloride was removed by vacuum. Once dried, the resulting powder was set up with 10 mL methanol and stirred for 2 h. After this time, methanol was removed by vacuum, the solid was washed with Milli-Q water for several times recovering the solid each time by centrifugation and then with methanol. Finally, it was filtered and dried. AC-6_EG was obtained by dispersing 200 mg of AC-6 in 10 mL acetonitrile with 100 µL ethylene glycol and 25 µL H₂SO₄ (J.T. Baker, 95-97%). The mixture was stirred and heated at 40 °C for 24 h. After that, it was washed with Milli-Q water for several times, decanting the liquid phase by centrifugation and solid recovered by filtration.

Characterization analysis

Elemental analyses were determined by using a Perkin-Elmer CHNOS analyser. ATR-FTIR spectra were acquired by using a Bruker Tensor27 instrument. The samples were placed in an oven at 100 °C for 12 h before recording the spectra in order to remove physisorbed water. Then, the samples were equilibrated at room temperature before the measurement was performed. Raman spectra were recorded at ambient temperature with a 514 nm laser excitation on a Renishaw In Via Raman spectrophotometer equipped with a CCD detector. XPS measurements were carried out in a SPECS spectrometer with a Phoibos 150 MCD-9 detector using a non-monochromatic X-ray source (Al and Mg) operating at 200 W. Spectra deconvolution was performed using the CASA software. The samples were submitted to vacuum in the pre-chamber of the spectrometer at $1 \cdot 10^{-9}$ mbar. Temperature-programmed desorption (TPD) coupled to a mass-spectrometer (TPD-MS) measurements

were carried out in a Micrometer II 21920 connected to a mass-spectrometer. In particular, the carbonaceous sample (100 mg) was heated from room temperature to 900 °C at 10 °C min⁻¹ under helium atmosphere. Zeta potential of aqueous suspension of the series of AC-X samples (5 mg) were measured in the pH range from 2 to 6 using a Zetasizer Malvern equipment.

Reaction procedure

In a typical experiment, 20 mg of the appropriate catalyst was dispersed by bath sonication (450 W sonicator) in 2 mL of ethanol in 25 mL round bottom flask. To this slurry, 1 mmol of styrene and 2 mmol of hydrazine hydrate were added. This reaction mixture was kept in a preheated oil bath maintained at 60 °C. This reaction mixture was stirred vigorously for the required time either under oxygen atmosphere or at air atmosphere as required.

Analytical measurements

From the reaction mixture, a known aliquot of the sample was periodically taken and injected in a gas chromatography to determine the kinetics of the reaction. The conversion of styrene was determined by gas chromatography using internal standard and the products formed in the reaction were confirmed using GC-MS.

Homogeneous catalytic tests

Homogeneous reactions were carried out as indicated above, but using benzoquinone, 9,10-anthraquinone, benzoic acid, hydroquinone or acetophenone as organocatalysts (0.1 mmol).

Results and Discussion

As catalysts in the present study, a commercial active carbon (Norit SX Ultra) was used as the parent material that was submitted to chemical oxidation by heating in concentrated aqueous nitric acid for various times. A series of three samples denoted as AC-X (X being the time of the nitric acid treatment in hours) was prepared. Table 1 summarizes

the elemental analysis of commercial AC submitted or not to the chemical treatment with nitric acid. It is well known in carbon chemistry that nitric acid introduced oxygenated functional groups on the surface of the active carbons, mainly ketone groups and hydroxyl and carboxylic acid groups.^{19, 20} The presence of these groups can be controlled by the time of the chemical oxidation and can be determined by chemical analysis and thermoprogrammed desorption (TPD).²¹⁻²³ As it can be seen in Table 1, combustion analysis shows that the longer the nitric acid treatment is, the larger the decrease in the carbon content is, going from about 75 to 61 % accompanied with a concomitant increase of the oxygen content. Also some minor increase in the nitrogen content was observed. This analytical data was in agreement with the expected effects of nitric acid treatment increasing oxygenated functional groups and producing some nitration of the AC sample.

Table 1. Elemental analyses (wt %) of commercial AC and nitric acid treated samples.				
Catalyst	N	C	H	O
AC ^a	0.38	75.30	0.37	23.95
AC-3 ^b	1.22	74.61	1.14	23.02
AC-6 ^b	1.37	72.34	0.66	25.63
AC-20 ^b	0.94	61.42	0.66	36.97
^a 0.23% of S was found for this sample. S was absent in the other samples; ^b The numbers 3, 6 and 20 represent the time of the nitric acid treatment.				

As expected, IR spectroscopy did not provide any relevant information due to the lack of transmission or reflectance for this type of material (see Figure S1 in the supporting information). Raman spectroscopy, on the other hand, showed the expected G and D bands accompanied with their corresponding overtones (2D, D+G) that appear at about 1600, 1350 cm⁻¹ and in the region 2600-3000 cm⁻¹, respectively.²⁴ These spectral features were maintained, although the bands became somewhat broader and less resolved, upon the nitric

acid treatment. As an example, Figure 1a presents the Raman spectra of AC and AC-6 to illustrate the type of minor changes observed in Raman spectroscopy.

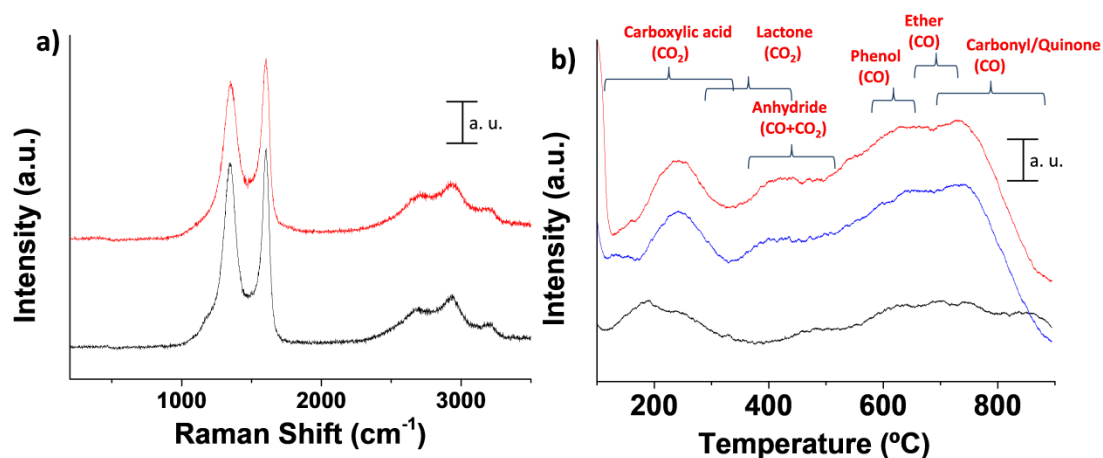


Figure 1. Raman spectra (a) and TPD analysis (b) for AC (black), AC-3 (blue) and AC-6 (red). Raman spectra and TPD plots have been shifted in the vertical scale for clarity. TPD graph includes peak assignment based on evolved gases (CO and CO₂) at different temperatures.

TPD is a very well established technique to discuss and quantify the nature of the oxygenated functional groups in active carbons.²³⁻²⁵ Upon heating these materials, a weight loss in the range from 100 to 350 °C associated to the evolution of CO₂ is ascribed to the decomposition anhydrides, carboxylic acids and lactones. Further heating results in additional weight loss in the range of temperature from 400 to 800 °C attributable to the decomposition of carbonyl groups.²³⁻²⁵ Figure 1b shows the TPD profile of three of the samples used in the present study to illustrate the profiles observed in the TPD and the changes occurring upon HNO₃ treatment, while Table 2 summarizes the estimation of the density of the oxygenated functional groups. As it can be seen there, in accordance with the role of nitric acid as oxidizing agent, the oxygen content and density of oxygenated functional group increases along the time of nitric acid treatment. This increase in the oxygen content is reflected in the higher intensity of the TPD curves, indicating higher CO₂ and CO evolution as the depth of

oxidation HNO_3 increases. Both the peaks corresponding to CO_2 evolution, exhibiting a maximum intensity at 240 °C and the ones due to CO evolution appearing as two peaks with maximum intensity about 630 and 740 °C, respectively, were observed together with an additional peak at intermediate temperatures with maximum intensity at 420 °C that corresponds to lactone and anhydride decomposition. According to the literature,²³ the peak of CO evolution peaking at lower temperature could be attributed to phenol like substructures on the AC treated material, while the high temperature CO evolution at 740 °C is ascribed to carbonyl groups and quinones. Overall TPD appears as a very convenient technique to follow surface oxidations caused by nitric acid by determining the area of the TPD plot and to address the type of oxygenated functional groups present in AC-X. The difference between the present AC and the other AC-X samples allow to discuss the effect of HNO_3 causing surface oxidation.

Table 2. Estimation of density functional groups for the different ACs based on the intensity of TPD plots. ^a						
Catalyst	Carboxylic acid (CO ₂), (a.u.)	Lactone (CO ₂), (a.u.)	Anhydride (CO ₂ +CO), (a.u.)	Phenol (CO), (a.u.)	Ether (CO), (a.u.)	Carbonyl /Quinone (CO), (a.u.)
AC	3	-	1	2	2	2
AC-3	10	1	7	4.5	5	10
AC-6	8	2.5	4.5	8	2.5	7
AC-20	3.5	6	15	4	5	9.5

^aQuantifications have been based on the signal provided by the instrument for the same amount of sample. The value of the arbitrary unit is indicated in the flat Figure 1.

XPS analysis was more informative respect to the changes occurring on the surface of AC upon nitric acid treatment.²⁴⁻²⁶ Basically the C1s peaks become broader upon nitric acid treatment and the contribution of carbon atoms bounded to oxygen increases upon treatment, as well as the intensity of the O1s peak (Figure S2). For comparison, Figure 2 shows the XPS C 1s and O 1s peaks recorded for AC and AC-6 to illustrate these changes that indicate that

nitric acid oxidation produces an increase in the O/C atomic percentage at the surface from 0.57 to 0.91 of oxygenated functional groups on the surface. Table 3 summarizes the XPS data of all the activated carbon samples under study.

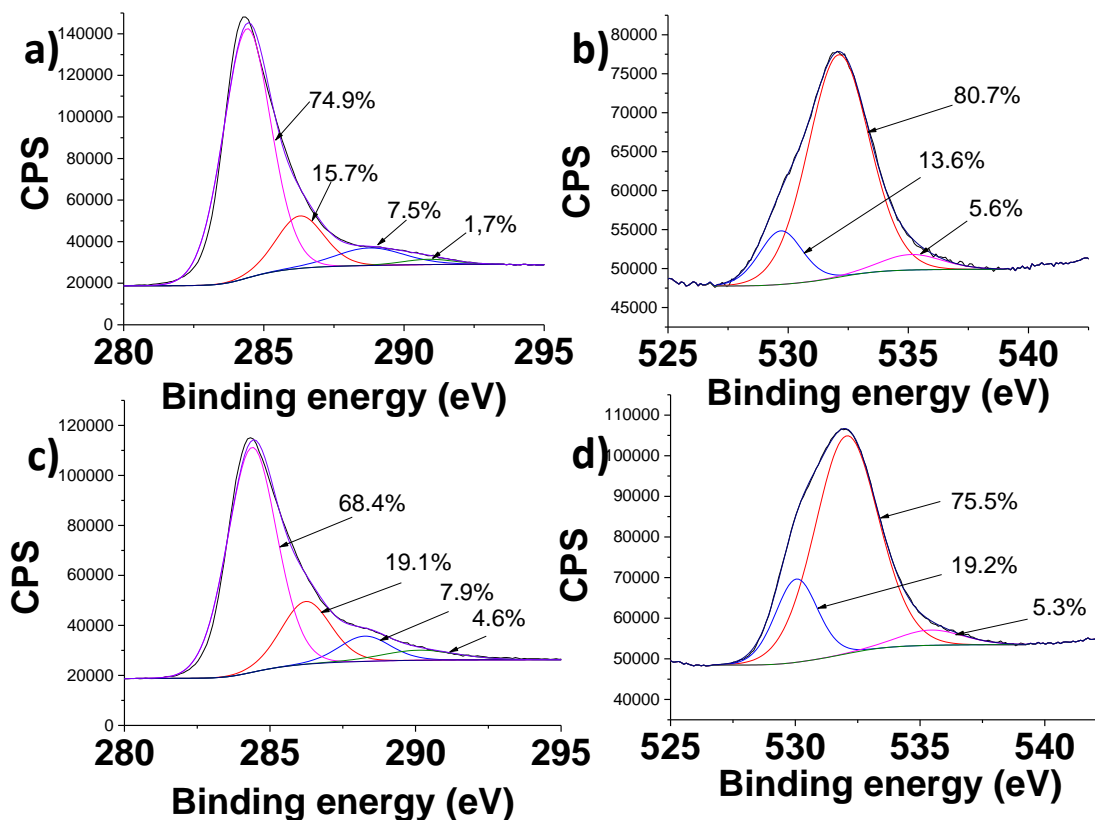


Figure 2. XPS spectra of C1s (a, c) and O1s (b, d) for AC (a, b) and AC-6 (c, d).

Catalyst	C1s				O1s		
	C=C	C-OH/ C-O-	C=O	COO	O-H/C- O-C	C=O	COO
AC	74.9	15.7	7.5	1.7	80.7	13.6	5.6
AC-3	71.8	13.1	9.6	5.4	31.0	62.3	6.7
AC-6	68.4	19.1	7.9	4.6	75.5	19.2	5.3
AC-20	62.8	26.1	6.7	4.4	36.6	36.6	26.8

Also in agreement with the generation of surface carboxylic acid groups in the treatment of AC with HNO₃, aqueous suspensions of AC-X shows increasing negative zeta potential as a function of the HNO₃ treatment time. Figure S16 shows zeta potential measurements for aqueous suspensions of AC-X in the range of pH values 2-6.

The set of AC samples prepared were screened with regard to their catalytic activity for hydrogenation of styrene by hydrazine. Figure 3 shows the temporal profile of styrene conversion, ethylbenzene being the only product observed in almost complete selectivity. This Figure shows that commercial active carbon already exhibits a good catalytic activity for styrene hydrogenation that is improved upon oxidation by nitric acid for 3 and 6 h, the most active samples being AC-6. It was also observed that prolonged oxidation treatment with nitric acid (20 h) is detrimental for the catalytic activity of this material.

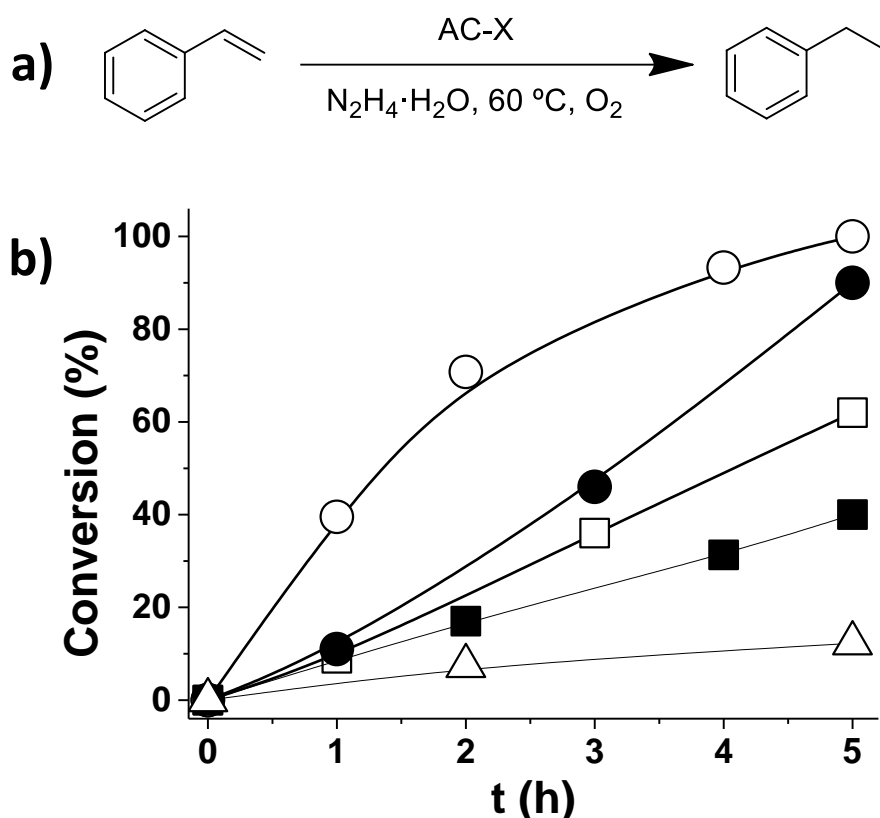


Figure 3. a) Catalytic styrene reduction to ethylbenzene and b) time conversion plots for the conversion of styrene to ethylbenzene showing the effect of HNO₃ treatment time over AC. Legend: AC (■), AC-3 (●), AC-6 (○), AC-20 (□) and in the absence of catalyst (Δ). Reaction

conditions: 20 mg catalyst, styrene (1 mmol), $\text{N}_2\text{H}_4\cdot\text{H}_2\text{O}$ (2 mmol), ethanol (2 mL), 60 °C, oxygen atmosphere.

Reusability of AC-6 as catalyst was checked by performing a series of consecutive reactions under the same conditions using the same sample recovered after each run by filtration, washed with ethanol and used in a subsequent run without further treatment. The time conversion plot for these consecutive uses is presented in Figure 4. It was observed that the catalytic activity of the material not only does not decrease, but even increases somewhat upon reuse. This increase in catalytic activity upon reuse could be due to an increase of the density of active sites upon exposure of the catalyst to hydrazine as reducing agent, without being deactivated under the reaction conditions. This suggestion would be compatible with the proposal of hydroquinone-type substructures as the catalytically reactive centres that will be presented below. In order to confirm this hypothesis, the six-fold used AC-6 material was characterised by XPS (Figure S3). Data analysis reveals that the used AC-6 material has been partially reduced and an increase of the O 1s band corresponding to hydroquinone-like moiety respect to the fresh material is observed (from 19.2 to 27.3 %).

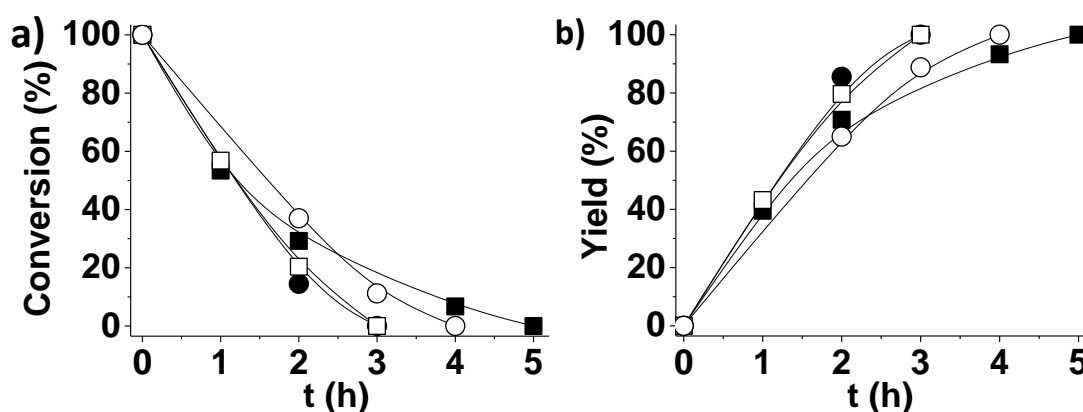


Figure 4. Time conversion plot for styrene (a) and ethylbenzene (b) using AC-6 as catalyst and showing the reusability of the material. Legend: First use (■), second use (●), fourth use (□), sixth use (○). Reaction conditions: 20 mg catalyst, styrene (1 mmol), $\text{N}_2\text{H}_4\cdot\text{H}_2\text{O}$ (2 mmol), ethanol (2 mL), 60 °C, oxygen atmosphere.

To put into context the catalytic activity of AC-6 respect to other carbon materials, a series of reactions were carried out under same experimental conditions using other carbon materials such as graphite, diamond NPs, MWCNT and even graphene. Graphite, diamond NPs and MWCNTs are commercial samples and were used as received. Graphene was prepared by pyrolysis of alginate powders at 900 °C under argon followed by exfoliation of the graphitic carbon residue as previously reported.¹⁸ The detailed characterization of graphite, diamond NPs, MWCNT and graphene by textural properties (Table S3), elemental (Table S4), Raman (Figure S11) and XPS (Figures S12-15) spectroscopic techniques in the supporting information. A comparison of the temporal profile for the styrene hydrogenation by hydrazine using these carbon materials is shown in Figure 5. As it can be seen in this Figure, AC-6 was the most active material compared to other carbon catalysts examined for this reaction. As it has been commented previously, to rationalize the influence of HNO₃ treatment on the catalytic activity of AC-X, the results of the different activity of the various carbon materials tested as catalysts, the most likely rationalization of the higher activity of AC-6 respect to other carbon samples is the higher density of adequate active sites to promote hydrazine decomposition resulting in the hydrogenation of styrene. In other words, HNO₃ treatment of AC and the surface oxidation caused by this acid generates oxygenated active sites that are present in larger quantities in AC-6 than in the other carbon materials.

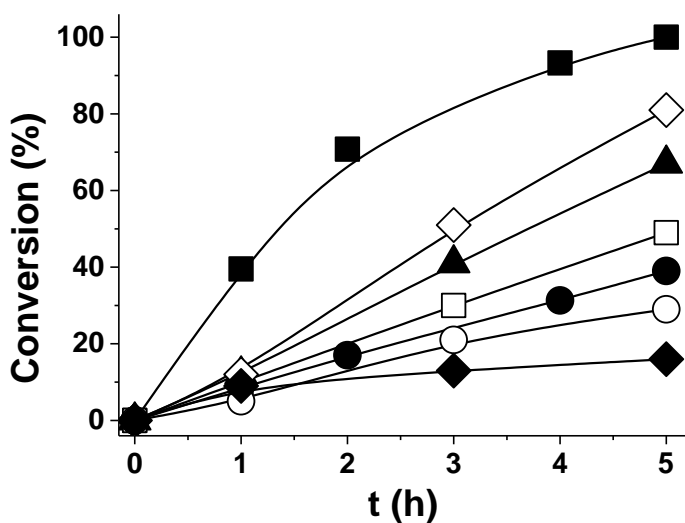


Figure 5. Time conversion plots for a series of carbon catalysts in the conversion of styrene to ethylbenzene using hydrazine hydrate under the optimal reaction conditions. Legend: AC-6 (■), AC (●), graphene (▲), MWCNT (□), diamond (◇), graphite (○), AC-6 under air atmosphere (◆). Reaction conditions: 20 mg catalyst, styrene (1 mmol), $\text{N}_2\text{H}_4\cdot\text{H}_2\text{O}$ (2 mmol), ethanol (2 mL), 60 °C, oxygen atmosphere.

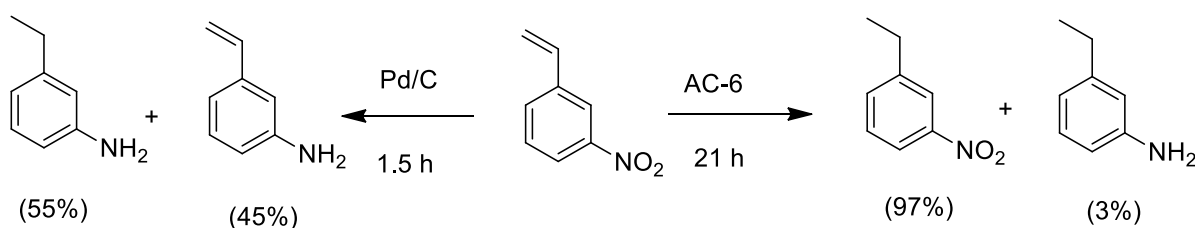
Concerning the reaction mechanism, it has been proposed that the hydrogenation reaction is initiated by the oxidation of hydrazine to diimide by molecular oxygen, diimide being spontaneously decomposed to hydrogen.²⁷⁻²⁹ To check this possibility, an analogous experiment under air instead of oxygen atmosphere was performed, observing a significant decrease in the catalytic activity of the material, which is in agreement with the role of oxygen to activate hydrazine (Figure 5).

The scope of the reaction was screened by carrying out the hydrogenation of a series of C=C double bonds by hydrazine using AC-6 as catalyst. The results are presented in Table 4. As it can be seen there, substituted styrenes having electron rich/poor substituents in the para/meta positions undergo also complete hydrogenation to their respective substituted ethylbenzenes. Other primary vinylic compounds either conjugate or with allylic substitution also undergo hydrogenation in almost complete conversion. Cis-cyclooctene becomes also

easily hydrogenated as well as terminal linear alkene. Disubstituted α -methylstyrene or t-stilbene also undergo hydrogenation to their corresponding dihydro products. Vinylcyclooctane and N-vinylcaprolactam also converted with complete selectivity to the corresponding saturated compounds. In the case of ethyl cinnamate, selectivity at complete conversion was not 100 % due to the observation of products derived from the attack of hydrazine to the substrate in some extent. As Table 4 shows, the two cases in where activity of AC-6 was lower correspond to cyclohexanol and disubstituted t-anethole. Overall, the data from this Table shows a wide scope and applicability of AC-6 as metal-free hydrogenation catalyst.

Table 4. Scope of AC-6 metal-free hydrogenation catalyst by hydrazine as reducing agent with different alkenes under the optimized reaction conditions. ^a				
Run	Alkene	Time (h)	Conversion (%) ^b	Selectivity (%) ^b
1	Styrene	7	100	100
2	4-Chlorostyrene	18	100	100
3	4-Methoxystyrene	9	100	100
4	Allyl phenyl sulphide	13	96	99
5	Allyl phenyl ether	24	82	99
6	Cis-cyclooctene	9	100	100
7	4-Fluorostyrene	6	100	100
8	3-Nitrostyrene	21	100	97(3) ^c
9	2-Vinylnaphthalene	7	100	100
10	1-Decene	7	100	100
11	α -Methylstyrene	16	100	100
12	t-Stilbene	7	100	100
13	Ethyl cinnamate	7	100	84
14	Allyl benzyl ether	7	100	100
15	t-Anethole	48	56	100
16	Vinylcyclooctane	14	100	100
17	N-Vinylcaprolactam	12	100	100
18	2-Cyclohexen-1-ol	32	38	98
^a Reaction conditions: alkene (1 mmol), AC-6 (20 mg), N ₂ H ₄ .H ₂ O (2 mmol), ethanol (2 mL), 60 °C, oxygen atmosphere.				
^b Determined by GC.				
^c Values in parenthesis correspond to the selectivity of 3-aminoethylbenzene.				

An additional issue was to compare the performance and selectivity of AC-6 in the chemoselective hydrogenation of 3-nitrostyrene. This substrate has been proposed as model compound in the case of Au catalysts to determine the preferential hydrogenation of C=C double bond versus nitro groups.^{30,31} In a related precedent, hydrogenation of 3-nitrostyrene was reported using ammonia/hydrazine treated AC³² at 100 °C and excess hydrazine.^{32, 33} It was observed that simultaneous hydrogenation of both (-NO₂ and C=C) functional groups with variant selectivity depending on the treatment. In the present study, hydrazine used was only two equivalents and may be for this reason as well as lower reaction temperature, better selectivity can be achieved. To further address, the chemoselectivity of AC-6 under the present reaction conditions, a control experiment using a commercial 10 wt% Pd/C sample as unselective catalyst was performed. A complete hydrogenation of the nitro group with about 50% reduction of C=C double bond under the reaction conditions was achieved using Pd/C. Scheme 1 compares the performance of Pd/C with respect to that of AC-6 showing that in contrast to the ammonia treated AC³² or Pd/C, the AC-6 sample exhibits a remarkable chemoselectivity for the hydrogenation of C=C double bond respect to the nitro group.



Scheme 1. Comparison of the activity of AC-6 with Pd/C in the reduction of 3-nitrostyrene.

The numbers in brackets correspond to the yield values for each product. Reaction conditions: 3-nitrostyrene (1 mmol), AC-6 (20 mg) or 10% Pd/C (10 mg), N₂H₄.H₂O (2 mmol), ethanol (2 mL), 60 °C, oxygen atmosphere.

When dealing with carbocatalysts, one important issue is to address the nature of the active sites. Information about the nature of the active sites can be obtained at least in two different ways, i.e. by using organic molecules as models of the possible substructures that

can be found on the carbocatalyst or by submitting the material to derivatization masking selectively certain groups that are presumed to play a catalytic role.¹³ In the present study we have followed those two approaches to learn more about the centres responsible for the catalysis and the results are presented in Figures 6 and 7. Thus Figure 6 compares the catalytic activity of AC-6 with that of the aromatic molecules such as benzoquinone, anthraquinone, hydroquinone, benzoic acid and acetophenone. As it can be seen there, all these organic molecules exhibit certain activity to promote styrene reduction to ethylbenzene by hydrazine. The most active one was, however, hydroquinone, but quinones, particularly anthraquinone, were also notably active. In the past, we have shown that quinone/hydroquinone redox pairs present on substructures on graphenes can act as active sites for hydrogen peroxide reduction.³⁴ In the present case it also makes sense that styrene reduction by hydrazine can also be promoted by this type of redox centres. However, the catalytic activity of other organic functional groups such as carboxylic acids and ketones is also revealed by Figure 6, although the last one was much less efficient. This opens the possibility that other substructures could also act as catalytic centres in hydrogenation by hydrazine.

In another series of experiments, the most active AC-6 sample was submitted to chemical derivatization trying to mask different oxygenated functional groups and determine the catalytic activity of these derivatives. Experimental section describes the recipes followed to obtain these derivatives, while the supporting information contains characterization data including elemental analyses, IR spectra, Raman, XPS and TPD for these three derivatives (Tables S1, S2 and Figures S4-S10). To determine the possible role of carboxylic acids, AC-6 was treated with thionyl chloride and, then, methanol to convert these functional groups selectively into the corresponding methyl esters (Sample AC-6_CO₂Me). TPD profile shows that after esterification, the peak of CO₂ evolution that appears at 240 °C present in AC-6

disappears and is replaced by a much broader and intense CO₂ peak corresponding to esters with maximum intensity at 350 °C. The ketonic groups were masked by reaction with benzylamine that should transform them into the corresponding benzylimines. This masking is clearly seen in the TPD profile, where the two peaks corresponding to CO evolution completely disappear (sample AC-6=NPh). Another sample was obtained by simultaneous masking of carboxylic acids and ketone groups (sample AC-6_CO₂Me, =NPh). Finally, the last AC-6 derivative was the sample obtained by treating AC-6 with ethylene glycol under acid catalysis that should form acetals of carbonylic groups and ethers of hydroxyls. In accordance to the expected derivatization AC-6_EG exhibits in TPD profile a shift in the peak of CO₂ evolution from 230 to 280 °C and some changes in the CO evolution. Styrene hydrogenation by hydrazine was also evaluated with these functionalized materials obtained by derivatization of AC-6, observing (see Figure 7) that the catalytic activity of AC-6 is significantly decreased by these derivatization treatments. These results are in agreement with the presumed role of carboxylic acids and ketones as active sites for the reduction of C=C double bonds using hydrazine in the literature.^{12, 17} These interpretations of the catalytic activity of the AC-6 sample are also in accordance with the significant activity of hydroquinone/quinone compounds presented in Figure 6.

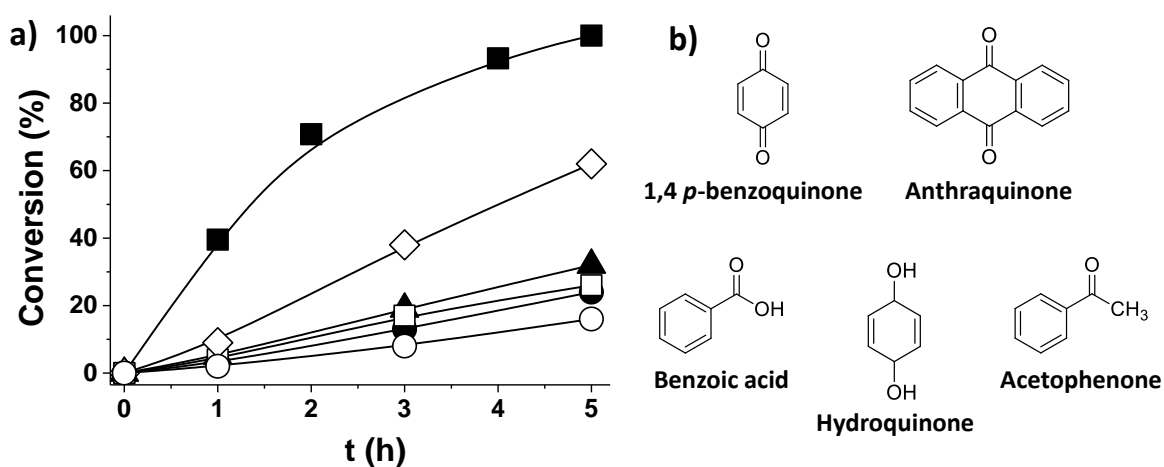


Figure 6. a) Time conversion plots for the conversion of styrene to ethylbenzene (a) using series of model compounds like benzoquinone, 9,10-anthraquinone, benzoic acid, hydroquinone and acetophenone. Legend: AC-6 (■), benzoquinone (●), anthraquinone (▲), benzoic acid (□), hydroquinone (◇), acetophenone (○) as heterogeneous/homogeneous catalyst. b) Organic molecules used as model compounds for possible active sites on AC. Reaction conditions: 20 mg catalyst/organocatalyst (0.1 mmol), styrene (1 mmol), $N_2H_4.H_2O$ (2 mmol), ethanol (2 mL), 60 °C, oxygen atmosphere.

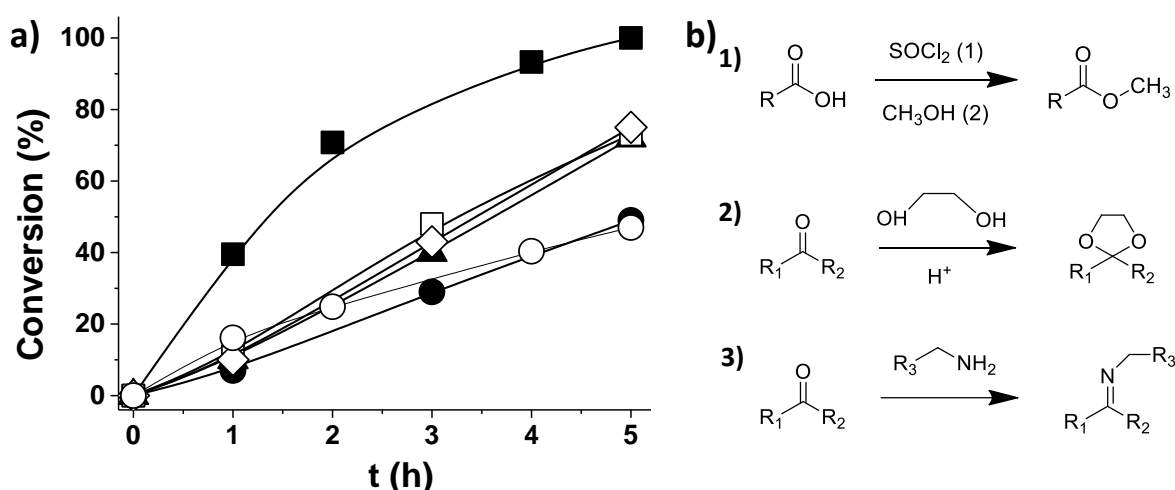


Figure 7. a) Comparison of time conversion plots for styrene to ethylbenzene using AC-6, AC-6 treated under argon atmosphere, masking with benzyl amine (NPh), reacted with ethylene glycol (EG) or with $SOCl_2$ and MeOH (CO_2Me). Legend: AC-6 (■), AC-6 under argon atmosphere (●), AC-6_EG (▲), AC-6=NPh (□), AC-6_CO₂Me (◇), AC-6CO₂Me, =NPh(○). b) Scheme illustrating the expected transformation of surface functional groups for the different treatments applied to AC-6. (1) thionyl chloride and methanol, (2) with ethyleneglycol, and (3) with benzylamine. Reaction conditions: 20 mg catalyst, styrene (1 mmol), $N_2H_4.H_2O$ (2 mmol), ethanol (2 mL), 60 °C, oxygen atmosphere.

Conclusions

In the present manuscript, it has been shown that the intrinsic catalytic activity of a commercial active carbon to promote hydrogenation of C=C double bonds by hydrazine can be tuned and increased by appropriate oxidative treatment with nitric acid. The most efficient sample is the one prepared by 6 h nitric acid treatment. The reaction requires oxygen to promote hydrazine oxidation to diimide. This active carbon has better performance than other carbon catalysts such as graphene, CNT, diamond and graphite, while exhibiting a wide scope. Compared to a conventional Pd/C catalyst, active carbon exhibits a significant chemoselective reduction of C=C versus nitro group. Comparison of the performance of nitric acid treated active carbon with organic compounds as models, as well as selective masking of functional groups suggest that hydroquinone groups are the most efficient catalytic centres promoting this reaction although other oxygenated functional groups also exhibit certain activity. Overall our data illustrates that modification of active carbons can be a useful strategy to obtain carbocatalysts with enhanced activity.

Supporting Information

Characterization of AC-6, AC-6_CO₂Me, AC-6=NPh, AC-6_CO₂Me, =NPh, AC-6_EG by TPD, ATR-IR, XPS, Raman methods. In addition, diamond, graphite, graphene and MWCNT were also characterized by elemental, Raman and XPS analysis.

Acknowledgements

SN thanks financial support by the Fundación Ramón Areces (XVIII Concurso Nacional para la Adjudicación de Ayudas a la Investigación en Ciencias de la Vida y de la Materia, 2016). AD thanks the University Grants Commission (UGC), New Delhi, for the award of an Assistant Professorship under its Faculty Recharge Programme. AD also thanks the Department of Science and Technology, India, for the financial support through Extra Mural Research Funding (EMR/2016/006500). Financial support by the Spanish Ministry of

Economy and Competitiveness (Severo Ochoa SEV2016-0683, Grapas and CTQ2015-69563-CO2-1) is gratefully acknowledged.

References

1. Ponec, V.; Bond, G. C., *Catalysis by metals and alloys*. Elsevier: 1995; Vol. 95.
2. Boudart, M., Heterogeneous catalysis by metals. *J. Mol.Catal.* **1985**, *30*, 27-38.
3. Sinfelt, J. H., Heterogeneous catalysis by metals. *Progress in solid state chemistry* **1975**, *10*, 55-69.
4. Jaouen, F.; Proietti, E.; Lefèvre, M.; Chenitz, R.; Dodelet, J.-P.; Wu, G.; Chung, H. T.; Johnston, C. M.; Zelenay, P., Recent advances in non-precious metal catalysis for oxygen-reduction reaction in polymer electrolyte fuel cells. *Energy Environ. Sci.* **2011**, *4*, 114-130.
5. Bullock, R. M., *Catalysis without precious metals*. John Wiley & Sons: 2011.
6. Dreyer, D. R.; Bielawski, C. W., Carbocatalysis: Heterogeneous carbons finding utility in synthetic chemistry. *Chem. Sci.* **2011**, *2*, 1233-1240.
7. Navalon, S.; Dhakshinamoorthy, A.; Alvaro, M.; Garcia, H., Carbocatalysis by graphene-based materials. *Chem. Rev.* **2014**, *114*, 6179-6212.
8. Chua, C. K.; Pumera, M., Carbocatalysis: the state of “metal-free” catalysis. *Chem. Eur. J.* **2015**, *21*, 12550-12562.
9. Mochida, I.; Korai, Y.; Shirahama, M.; Kawano, S.; Hada, T.; Seo, Y.; Yoshikawa, M.; Yasutake, A., Removal of SO_x and NO_x over activated carbon fibers. *Carbon* **2000**, *38*, 227-239.
10. Sumathi, S.; Bhatia, S.; Lee, K.; Mohamed, A., Selection of best impregnated palm shell activated carbon (PSAC) for simultaneous removal of SO₂ and NO_x. *J. Hazardous Mater.* **2010**, *176*, 1093-1096.
11. Su, D. S.; Zhang, J.; Frank, B.; Thomas, A.; Wang, X.; Paraknowitsch, J.; Schlögl, R., Metal-Free Heterogeneous Catalysis for Sustainable Chemistry. *ChemSusChem* **2010**, *3*, 169-180.
12. Navalon, S.; Dhakshinamoorthy, A.; Alvaro, M.; Antonietti, M.; Garcia, H., Active sites on graphene-based materials as metal-free catalysts. *Chem. Soc. Rev.* **2017**, *46*, 4501-4529.
13. Primo, A.; Parvulescu, V.; Garcia, H., Graphenes as Metal-Free Catalysts with Engineered Active Sites. *J. Phys. Chem. Lett.* **2017**, *8*, 264-278.
14. Su, D. S.; Perathoner, S.; Centi, G., Nanocarbons for the development of advanced catalysts. *Chem. Rev.* **2013**, *113*, 5782-5816.
15. Wu, S.; Wen, G.; Liu, X.; Zhong, B.; Su, D. S., Model molecules with oxygenated groups catalyze the reduction of nitrobenzene: Insight into carbocatalysis. *ChemCatChem* **2014**, *6*, 1558-1561.
16. Gao, Y.; Ma, D.; Wang, C.; Guan, J.; Bao, X., Reduced graphene oxide as a catalyst for hydrogenation of nitrobenzene at room temperature. *Chem. Commun.* **2011**, *47*, 2432-2434.
17. Larsen, J. W.; Freund, M.; Kim, K. Y.; Sidovar, M.; Stuart, J. L., Mechanism of the carbon catalyzed reduction of nitrobenzene by hydrazine. *Carbon* **2000**, *38*, 655-661.
18. Primo, A.; Sanchez, E.; Delgado, J. M.; Garcia, H., High-yield production of N-doped graphitic platelets by aqueous exfoliation of pyrolyzed chitosan. *Carbon* **2014**, *68*, 777-783.
19. Noh, J. S.; Schwarz, J. A., Effect of HNO₃ treatment on the surface acidity of activated carbons. *Carbon* **1990**, *28*, 675-682.
20. Rogaski, C.; Golden, D.; Williams, L., Reactive uptake and hydration experiments on amorphous carbon treated with NO₂, SO₂, O₃, HNO₃, and H₂SO₄. *Geophys. Res. Lett.* **1997**, *24*, 381-384.
21. Lopez-Ramon, M. V.; Stoeckli, F.; Moreno-Castilla, C.; Carrasco-Marin, F., On the characterization of acidic and basic surface sites on carbons by various techniques. *Carbon* **1999**, *37*, 1215-1221.

22. Zhou, J.-H.; Sui, Z.-J.; Zhu, J.; Li, P.; Chen, D.; Dai, Y.-C.; Yuan, W.-K., Characterization of surface oxygen complexes on carbon nanofibers by TPD, XPS and FT-IR. *Carbon* **2007**, *45*, 785-796.
23. Figueiredo, J.; Pereira, M.; Freitas, M.; Orfao, J., Modification of the surface chemistry of activated carbons. *Carbon* **1999**, *37*, 1379-1389.
24. Luo, J.; Liu, Y.; Wei, H.; Wang, B.; Wu, K.-H.; Zhang, B.; Su, D. S., A green and economical vapor-assisted ozone treatment process for surface functionalization of carbon nanotubes. *Green Chem.* **2017**, *19*, 1052-1062.
25. Ortega, K. F.; Arrigo, R.; Frank, B.; Schlögl, R.; Trunschke, A., Acid-Base Properties of N Doped Carbon Nanotubes: A Combined Temperature-Programmed Desorption, X ray Photoelectron Spectroscopy, and 2 Propanol Reaction Investigation. *Chem. Mater.* **2016**, *28*, 6826-6839.
26. Duong-Viet, C.; Liu, Y.; Truong-Phuoc, H. B. L.; Baaziz, W.; Nguyen-Dinh, L.; Nhut, J.-M.; C., P.-H., Carbon nanotubes containing oxygenated decorating defects as metal-free catalyst for selective oxidation of H₂S. *Appl. Catal. B: Environ.* **2016**, *191* 29-41.
27. Kumarraja, M.; Pitchumani, K., Simple and efficient reduction of nitroarenes by hydrazine in faujasite zeolites. *Appl. Catal. A: Gen.* **2004**, *265*, 135-139.
28. Ratnayake, W.; Grossert, J.; Ackman, R., Studies on the mechanism of the hydrazine reduction reaction: Applications to selected monoethylenic, diethylenic and triethylenic fatty acids of cis configurations. *J. Am. Oil Chemists Soc.* **1990**, *67*, 940-946.
29. Dhakshinamoorthy, A.; Alvaro, M.; Garcia, H., , , (14-15), , Metal-Organic Frameworks (MOFs) as Heterogeneous Catalysts for the Chemoselective Reduction of Carbon-Carbon Multiple Bonds with Hydrazine. *Adv. Synth. Catal.* **2009**, *351*, 2271-2276.
30. Corma, A.; Serna, P., Chemoselective hydrogenation of nitro compounds with supported gold catalysts. *Science* **2006**, *313*, 332-334.
31. Boronat, M.; Concepción, P.; Corma, A.; González, S.; Illas, F.; Serna, P., A molecular mechanism for the chemoselective hydrogenation of substituted nitroaromatics with nanoparticles of gold on TiO₂ catalysts: A cooperative effect between gold and the support. *J. Am. Chem. Soc.* **2007**, *129*, 16230-16237.
32. Fujita, S.-i.; Watanabe, H.; Katagiri, A.; Yoshida, H.; Arai, M., Nitrogen and oxygen-doped metal-free carbon catalysts for chemoselective transfer hydrogenation of nitrobenzene, styrene, and 3-nitrostyrene with hydrazine. *J. Mol. Catal. A: Chem.* **2014**, *393*, 257-262.
33. Fujita, S.-i.; Asano, S.; Arai, M., Nitrobenzene-assisted reduction of phenylacetylene with hydrazine over nitrogen-doped metal-free activated carbon catalyst: Significance of interactions among substrates and catalyst. *J. Mol. Catal. A: Chem.* **2016**, *423*, 181-184.
34. Espinosa, J. C.; Navalón, S.; Primo, A.; Moral, M.; Sanz, J. F.; Álvaro, M.; García, H., Graphenes as Efficient Metal-Free Fenton Catalysts. *Chem. Eur. J.* **2015**, *21*, 11966-11971.